Journal of Human Centered Technology

https://www.humentech.utm.my E-ISSN: 2821-3467

Enhanced Alzheimer's Disease Detection Using Transformer-Based GAN and Deep Learning Techniques

Ibrahem Mohammed Madhat[1*], Farhan Mohamed[2], Omar Albebashy[1] Ahmed Azzawi[1] Aminu Dau[3]

[1]Office Affairs Department of the University of Technology, Baghdad, Iraq
[2]Department of Computer Science, Universiti Teknologi Malaysia
[3]Department of Computer Science, Alqalam University Katsina, Nigeria

*Corresponding author ibrahem.m.madhat@uotechnology.eduiq

Cite: https://doi.org/10.11113/humentech.v5n2.139

Research Article

Abstract:
Early detection of Alzheimer's Disease (AD) is essential for timely clinical intervention. However, conventional Magnetic Resonance Imaging-based (MRI-based) diagnostic approaches are often limited by class imbalance, insufficient training data, inter-dataset variability, and inadequate feature extraction capability, which reduce the reliability of early-stage AD identification. This study proposed an enhanced deep learning framework that integrated a Transformer-based Generative Adversarial Network (TGAN) with an attention-enhanced ResNet-50 architecture for robust multiclass classification of Cognitively Normal (CN), Mild Cognitive Impairment (MCI), and Alzheimer's Disease (AD) MRI images. The TGAN model was employed to generate anatomically realistic synthetic MRI scans to address dataset imbalance and improve feature diversity, while the enhanced ResNet-50 utilized residual learning and attention mechanisms to improve the extraction of discriminative neuroanatomical features associated with disease progression. A comprehensive preprocessing pipeline was applied to standardize MRI data obtained from the ADNI and OASIS datasets. We conducted a series of experiments on the ADNI and OASIS databases. The proposed system demonstrated a classification accuracy of 94.8% on ADNI and 93.6% on OASIS, greatly surpassing baseline models such as ordinary ResNet-50, DenseNet-121, and traditional GAN-augmented CNNs. Ablation investigations further verified the significance of the Transformer-based generator and attention-enhanced residual blocks, each yielding substantial performance enhancements.

Keywords: Alzheimer's Disease detection; Transformer-based GAN; ResNet-50; Deep learning

1. INTRODUCTION

Alzheimer's Disease (AD) is a degenerative neurological disorder and the most common cause of dementia worldwide, accounting for approximately 60–70% of all dementia cases (1). Its impact on cognitive function and daily living activities necessitates early and accurate diagnosis (2). According to the World Health Organization, the number of individuals living with dementia is expected to reach nearly 150 million by 2050, placing enormous pressure on healthcare systems globally (3). Early diagnosis of AD is crucial because it enables timely and appropriate treatment. However, early-stage diagnosis remains challenging due to the complex structural abnormalities present in the brain. Magnetic Resonance Imaging (MRI) has emerged as one of the most reliable non-invasive imaging modalities for detecting structural brain abnormalities associated with AD (4). Deep learning-based techniques have demonstrated significant potential in automating AD detection from MRI scans (5). Convolutional Neural Networks (CNNs) have achieved competitive performance compared with handcrafted approaches. Nevertheless, the practical deployment of these models faces several important challenges: (1) high-quality annotated MRI datasets are limited due to privacy concerns and the difficulty of collecting balanced samples; (2) variations in scanner technology and demographic distributions across datasets reduce model generalizability; and (3) CNN-based classifiers often fail to capture long-range dependencies in brain structures and may overfit when trained on small datasets.

To address these challenges, this study proposed a deep learning-based architecture for AD detection that integrates preprocessing, data augmentation, and enhanced classification. Specifically, the proposed method employs a Transformer-based Generative Adversarial Network (TGAN) for data augmentation to generate high-quality and anatomically realistic MRI scans. Unlike conventional CNN-based generators, the transformer-based architecture effectively models long-range dependencies and contextual brain structures. These synthetic scans expand the dataset and mitigate class imbalance. For classification, we employ an Enhanced ResNet-50 architecture augmented with attention mechanisms and improved residual connections. The proposed framework was validated using two widely used benchmark datasets: the Alzheimer's Disease Neuroimaging Initiative (ADNI) (6) and the Open Access Series of Imaging

Received 08 March 2026; Accepted 03 June 2026
Available online 06 August 2026

Studies (OASIS) (7). Therefore, through this study, a comprehensive preprocessing pipeline incorporating skull stripping, bias field correction, normalization, and scan slicing to produce high-quality MRI inputs was designed, an enhanced TGAN-based MRI augmentation framework capable of generating realistic synthetic data to address data scarcity and improve class balance was proposed, and Enhanced ResNet-50 classifier integrated with attention mechanisms to improve the classification performance of AD, Mild Cognitive Impairment (MCI), and Cognitively Normal (CN) subjects was introduced.

Despite the rapid advancement of deep learning in medical image analysis, AD detection remains constrained by two interrelated challenges: limited data availability and weak model generalization. Most state-of-the-art classification models, including CNNs, depend heavily on large and balanced datasets to achieve robust performance (8). However, publicly available MRI datasets such as ADNI and OASIS are relatively small and imbalanced, which negatively affects classification accuracy (9). Furthermore, although traditional GAN-based augmentation methods have shown promise, they often struggle to generate anatomically realistic MRI scans. Standard convolutional generators are unable to effectively capture long-range spatial correlations among brain regions, which are essential for identifying subtle AD-related abnormalities. As a result, the generated synthetic images may contain unrealistic artifacts. Therefore, there is a need for a more robust generative framework capable of preserving global brain context. Motivated by these limitations, this study presents a TGAN for high-quality MRI data augmentation and an Enhanced ResNet-50 model with attention mechanisms and improved residual learning for classification. Together, these components address the two major challenges in AD detection: (i) data scarcity through the generation of anatomically consistent synthetic MRI scans, and (ii) improved classification robustness through attention-driven feature learning.

2. RELATED WORKS

In recent years, the diagnosis and classification of AD using neuroimaging and machine learning techniques have been extensively studied (10, 11). This section reviews prior research efforts in three key areas relevant to the proposed work: (1) deep learning-based AD classification in medical imaging, (2) data augmentation techniques, and (3) GAN-based image synthesis. Deep learning-based models such as Convolutional Neural Networks (CNNs) have demonstrated significant success in medical imaging tasks (12). In AD research, CNNs are widely applied to classify MRI and PET images into cognitive stages such as normal control (NC), mild cognitive impairment (MCI), and AD (13). Several studies have reported strong results using CNN-based approaches. For example, AbdulAzeem *et al.* (14) proposed a CNN architecture consisting of three convolutional and max-pooling layer pairs for binary AD classification. The proposed model was evaluated on MRI datasets and achieved 95.6% accuracy. Al-Khuzaie *et al.* (15) developed AlzNet, a five-layer CNN trained on 15,200 OASIS MRI scans. The model utilized the Adadelta optimizer with a 20% dropout rate and attained 99.53% accuracy. Al-Adhaileh *et al.* (16) compared AlexNet and ResNet50 on a four-class Kaggle dataset, where AlexNet achieved 94.53% accuracy compared with 58.07% for ResNet50. Antony *et al.* (17) evaluated VGG16 and VGG19 on 780 ADNI MRI images, reporting accuracies of 81% and 84%, respectively. Savaş *et al.* (18) benchmarked 29 pre-trained models on ADNI images and identified EfficientNetB0 as the best-performing model with 92.98% accuracy. In another study, Sarasua *et al.* (19) proposed a ResNet-Self-based approach to enhance hippocampal feature representation on ADNI datasets. Similarly, (20) combined parallel CNN feature extractors with ensemble learning for 3D MRI volumes. Ebrahimi *et al.* (21) applied a transfer learning-based approach to optimize ResNet features for limited datasets, while Khan *et al.* (22) employed deep feature extraction with external classifiers to improve cross-site generalization. Despite these advancements, several challenges remain in existing methods, including overfitting on limited datasets and difficulty in distinguishing subtle anatomical variations, which often lead to misclassification.

To address data scarcity and class imbalance in medical imaging, researchers have increasingly adopted GANs to generate realistic synthetic images (23). Although the original vanilla GAN demonstrated the feasibility of image generation, it is now rarely used in its basic form due to training instability. Nevertheless, it laid the foundation for numerous improved variants. Deep Convolutional GAN (DCGAN) (24) replaced fully connected layers with convolutional layers, enabling more effective spatial feature learning. A study by Abdelhalim *et al.* (25) introduced the Wasserstein distance as a loss function, thereby stabilizing training and improving gradient flow. StyleGAN (26), which builds upon Progressive Growing GAN (PGGAN) (27), introduced a mapping network to control image style and fine-grained features. In medical imaging applications, synthetic image generation often requires adherence to specific anatomical constraints. Conditional GANs (cGANs) (28) extend vanilla GANs by conditioning both the generator and discriminator on additional information such as class labels, paired or unpaired images, masked regions, or attention heatmaps. Pix2Pix (29) remains one of the most widely used cGAN architectures, employing a U-Net-based generator with skip connections and a patch discriminator to improve local image details. Its extensions, such as SRGAN (30), incorporate perceptual loss functions to further enhance high-frequency details. However, paired training data are often limited in clinical settings. To overcome this limitation, CycleGAN (31) enables unpaired image-to-image translation through cycle-consistency constraints, making it particularly useful for denoising tasks and domain harmonization. More advanced GAN-based models, such as StarGAN (32), support simultaneous translation across multiple domains within a single network. Oraby *et al.* (33) integrated GAN-based outputs with CNN classifiers to improve AD classification accuracy. Despite these improvements, conventional GANs still face several limitations, including the inability to consistently generate anatomically diverse and high-fidelity brain structures. These challenges have motivated increasing interest in transformer-based GAN architectures, which are better suited for capturing long-range dependencies in brain anatomy while maintaining stable adversarial training dynamics.

3. PROPOSED METHOD

The proposed framework is designed based on three main stages. First, a preprocessing pipeline is developed to ensure high-quality and anatomically consistent MRI inputs. The preprocessing stage includes skull stripping, bias field correction, intensity normalization, sagittal slice removal, and scan slicing. Second, data augmentation is performed using a GAN to address the limited availability and class imbalance commonly found in medical imaging datasets. The proposed GAN incorporates a Transformer-based Generator capable of capturing long-range relationships within MRI structures to generate anatomically realistic images. In addition, a Spectrally Normalized Discriminator with residual blocks is employed to stabilize adversarial training and reduce the generation of unrealistic artifacts. Furthermore, attention-enhanced feature encoding guides the generator to focus on diagnostically relevant brain regions. Finally, classification is performed using an Enhanced ResNet-50 model, which extends the standard residual network with attention mechanisms and improved skip connections. Figure 1 illustrates the proposed framework.

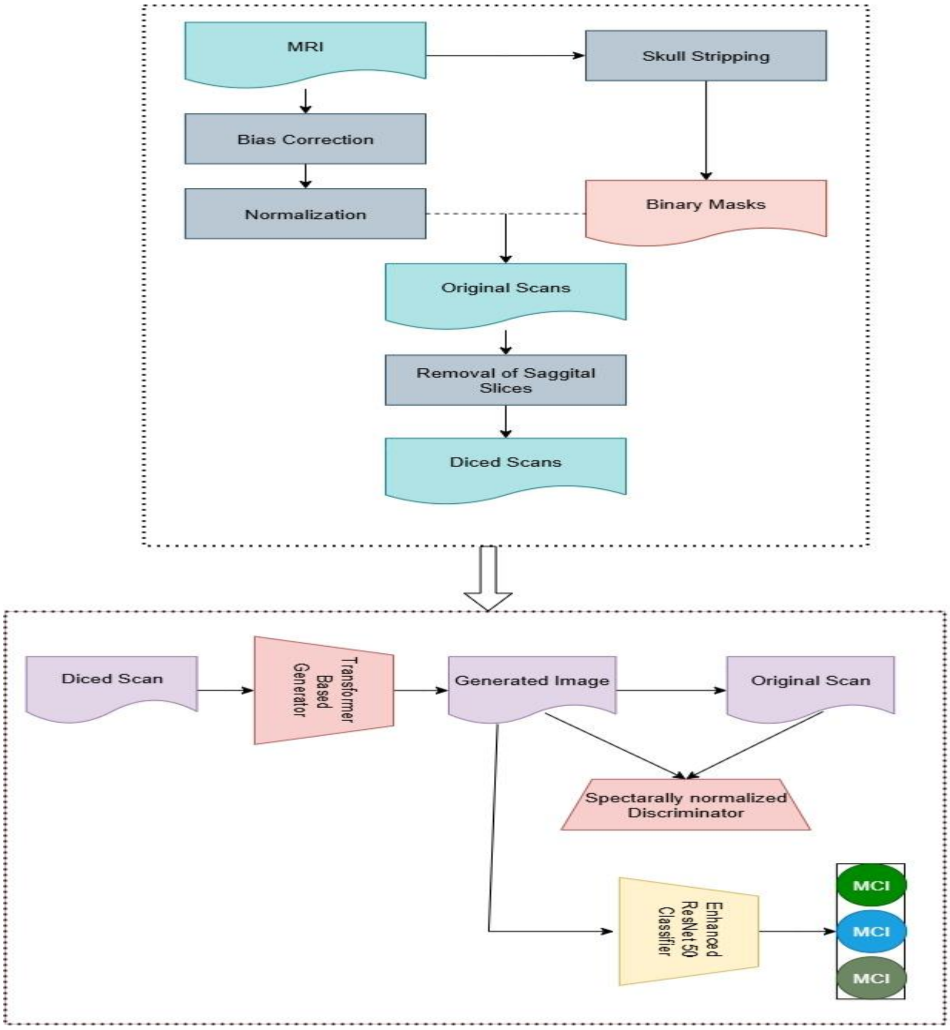

Figure 1. Conceptual diagram of the proposed framework.

3.1 Preprocessing Pipeline

As described earlier, the first stage involves a preprocessing pipeline, which plays a vital role in MRI data preparation. Generally, raw MRI data may contain non-brain tissues and spatial irregularities that can negatively affect feature extraction. To address these issues, multiple preprocessing operations are applied sequentially. Initially, skull stripping is performed to remove non-brain structures such as the skull, scalp, and other irrelevant features. This is followed by bias field correction to address intensity inhomogeneities caused by the scanner. Next, intensity normalization is applied to standardize voxel intensity distributions across subjects. To further improve the data quality, sagittal slice reduction is performed to eliminate unnecessary slices. In addition, scan slicing is conducted to partition each MRI volume into anatomically consistent slices. Finally, all preprocessed scans are resized to a uniform spatial resolution to match the input requirements of both the TGAN and the Enhanced ResNet-50 classifier.

3.2 Enhanced GAN for Data Augmentation

Following the preprocessing stage, the next step focuses on data augmentation using a TGAN. This component addresses the inherent limitations of medical imaging datasets, such as limited sample size and class imbalance, by generating high-quality synthetic MRI scans. Unlike conventional GAN architectures that rely primarily on convolutional layers, the proposed TGAN employs a Transformer-based Generator to capture long-range spatial dependencies and maintain structural consistency. In addition, it utilizes a Spectrally Normalized Discriminator with residual blocks to ensure stable adversarial

https://doi.org/10.11113/humentech.v5n2.139

training and reduce the risk of generating unrealistic artifacts. Details of the proposed TGAN generator and discriminator are presented in the following subsections.

3.3 Enhanced Transformer-Based Generator

Traditional GAN generators rely heavily on stacked convolutional layers, which are often insufficient for capturing global interactions across complex neuroanatomical structures. To address these limitations, the proposed Enhanced GAN incorporates a fully transformer-based generator for MRI synthesis. This generator introduces several architectural innovations: (1) Hierarchical Resolution Enhancement, in which high-resolution MRIs are progressively reconstructed using PixelShuffle-based upsampling; and (2) Transformer Encoder Blocks, where each refinement stage consists of stacked transformer encoder blocks composed of Multi-Head Self-Attention to model global dependencies between distant brain regions, feedforward MLPs with GELU activation (33) to introduce non-linearity and improve representational capacity, as well as Layer Normalization and residual connections. Inspired by the Vision Transformer (ViT) (34), the generator processes MRI images as tokenized feature patches rather than on a pixel-by-pixel basis, thereby significantly reducing computational complexity while preserving spatial coherence. In addition, dropout layers are incorporated within the transformer-based blocks to reduce overfitting. Figure 2 illustrates the proposed transformer-based generator.

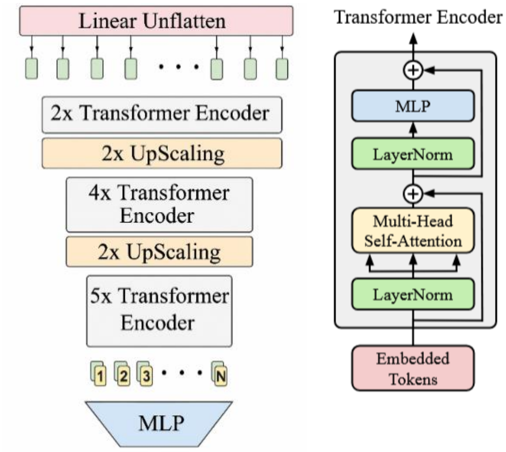

Figure 2. Illustration of the proposed transformer-based generator. While the transformer consists of multiple up-sampling stages combined.

3.3.1 Spectrally Normalized Discriminator

Complementing the generator, the discriminator is meant to discriminate between actual and synthetic MRIs data. The model includes a lightweight convolutional backbone supplemented with Spectral Normalization and Residual Blocks. The Spectral Normalization is applied to all convolutional layers (35), to prevent gradient explosion and mode collapse, two typical errors in medical GAN training. This results to smoother adversarial dynamics and improved convergence. Residual Blocks, are integrated to support deeper architectures without degradation. ReLU Activations and Average Pooling are employed for better efficiency. The average pooling is used to replace max pooling to reduce overfitting and maintain balance. Figure 3 shows the normalized descriminator.

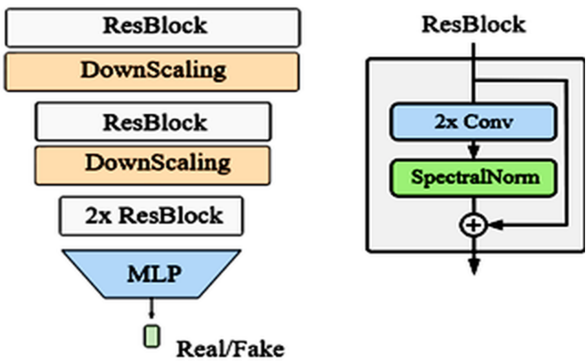

Figure 3. Normalized Discriminator.

3.3.2 Enhanced ResNet-50 for Classification

While the preprocessing pipeline guarantees that input data are anatomically coherent and the GAN augmentation enriches the dataset with structurally realistic synthetic MRIs, accurate diagnosis hinges on a classifier capable of extracting subtle disease-related signals. Standard convolutional networks, including the baseline ResNet-50, have showed potential in medical imaging; nevertheless, they often fail to identify the fine-grained neuroanatomical differences that define early Alzheimer's progression. To address this shortcoming, the Enhanced ResNet-50 combines various architectural enhancements targeted at amplifying diagnostic sensitivity, and lowering overfitting: The proposed model retains the core residual learning principle of ResNet-50, where shortcut connections allow the network to learn residual mappings instead of direct feature transformations. The residual operation is mathematically expressed as in Equation (1):

$$y = F(x, \{W_i\}) + x \tag{1}$$

where x denotes the input feature map, $F(x, \{W_i\}) +$ represents the residual mapping learned by convolutional layers with weights $\{W_i\}$, and y is the output feature representation. The shortcut connection improves gradient propagation, mitigates vanishing gradient problems, and enables stable training of deeper networks.

To improve the extraction of disease-specific biomarkers, attention modules were integrated into the residual blocks. The attention mechanism enables the network to assign higher importance to discriminative brain regions such as the hippocampus and cortical areas associated with Alzheimer's Disease progression. The channel attention process can be represented as in Equation (2):

$$\hat{X}_c = s_c \cdot X_c \tag{2}$$

where X_c is the input feature channel, s_c the learned attention coefficient, and $\hat{X}_c$ represents the recalibrated feature map. This operation suppresses irrelevant features while amplifying diagnostically meaningful patterns, thereby improving classification sensitivity and specificity.

Batch normalization layers were incorporated to stabilize training and reduce internal covariate shift by normalizing intermediate feature distributions. Dropout regularization was further introduced to reduce overfitting by randomly deactivating neurons during training, thereby improving model generalization across heterogeneous MRI datasets. Instead of using large fully connected layers, Global Average Pooling (GAP) was employed to reduce the number of trainable parameters and minimize overfitting. GAP summarizes spatial feature representations into compact global descriptors while preserving discriminative information relevant for classification. The final classification stage employs a softmax activation function to estimate the probability distribution across the three diagnostic classes: Cognitively Normal (CN), Mild Cognitive Impairment (MCI), and Alzheimer's Disease (AD). The softmax function is defined as in Equation (3):

$$P(y_i) = \frac{e^{z_i}}{\sum_{j=1}^{K} e^{z_j}} \tag{3}$$

where $P(y_i)$ is the predicted probability for class i, z_i denotes the output logits, and K represents the total number of classes.

4. EXPERIMENTAL METHOD

In this section, we explain the experimental study for evaluating the proposed model. We first describe the datasets then the experimental setting for the model evaluation. Next we presents the evaluation metrics.

4.1 Dataset Description

Experiments were conducted on a system equipped with an NVIDIA Tesla V100 GPU and an Intel Xeon 64-core processor. The model was implemented using PyTorch (36) and TensorFlow (37), and trained with the Adam optimizer (38). This study utilized two publicly available benchmark neuroimaging datasets, namely the Alzheimer's Disease Neuroimaging Initiative (ADNI) dataset (39) and the Open Access Series of Imaging Studies (OASIS) dataset, (40) to evaluate the effectiveness and generalization capability of the proposed framework for Alzheimer's Disease (AD) classification. The datasets contain T1-weighted brain MRI scans representing three diagnostic categories: Cognitively Normal (CN), Mild Cognitive Impairment (MCI), and Alzheimer's Disease (AD). To ensure consistency in data preparation, MRI volumes from both datasets were preprocessed and converted into two-dimensional sagittal slices. Approximately 3,000 MRI slices were extracted from the selected patient scans after preprocessing, including skull stripping, bias field correction, intensity normalization, and spatial resizing. The extracted slices were then grouped according to their corresponding diagnostic labels. The patient distribution and class balance were carefully considered to minimize classification bias and improve model robustness. Since the original datasets exhibited class imbalance, particularly for the MCI category, the proposed Transformer-based Generative Adversarial Network (TGAN) was employed to generate synthetic MRI images for minority classes and improve intra-class diversity. Table 1 shows the statistics of the datasets. Figures 4 and 5 show illustration of the ADNI and OASIS datasets respectively.

Table 1. Patient Distribution and Class Balance.

Dataset	Class	Number of Patients	Number of MRI Slices	Percentage (%)
ADNI	CN	42	620	20.7
	MCI	48	890	29.7
	AD	40	590	19.6
OASIS	CN	28	320	10.7
	MCI	30	340	11.3
	AD	24	240	8.0
Total	—	212	3,000	100

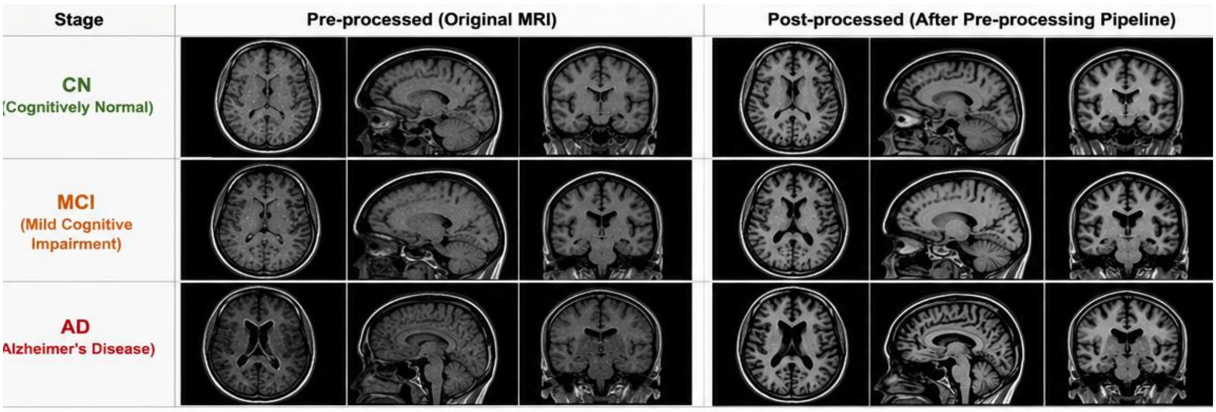

Figure 4. An illustration of the ADSNI datasets.

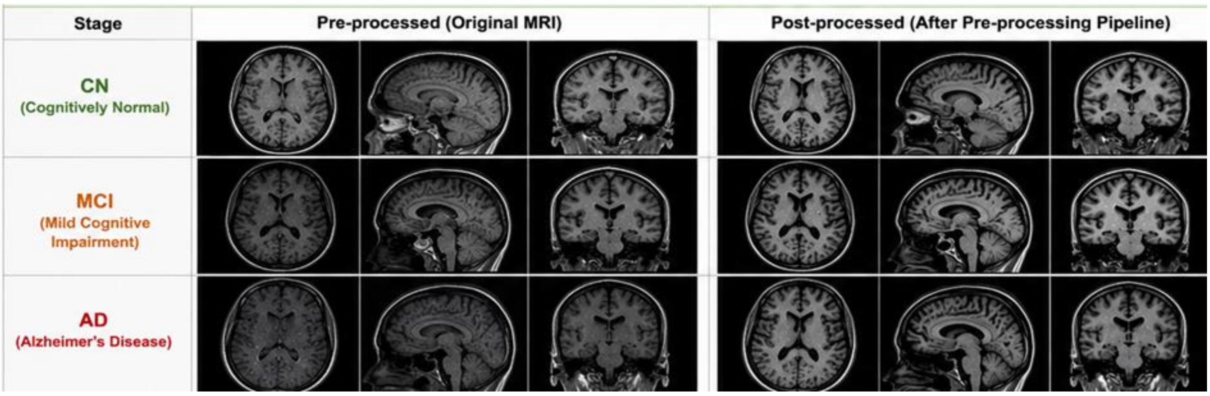

Figure 5. Illustration of OASIS datasets.

4.2 Hyperparameter Settings

The proposed model robustness was evaluated using five-fold cross-validation across different data splits. Table 3 shows the summary of the hyper parameter settings.

Table 2. Hyperparameter settings and MRI preprocessing configuration.

Category	Parameter	Value / Configuration
Hardware	GPU	NVIDIA Tesla V100
	CPU	Intel Xeon 64-Core
Frameworks	Deep Learning Libraries	PyTorch, TensorFlow
MRI Preprocessing	Skull Stripping	FreeSurfer / FSL BET
	Bias Field Correction	N4 Bias Correction
	Intensity Normalization	Min-Max Normalization
	Noise Reduction	Gaussian Filtering
	Spatial Resizing	224 × 224 pixels
	Slice Extraction	Sagittal MRI slices
Training Settings	Optimizer	Adam
	Learning Rate	0.0001
	Batch Size	32
	Number of Epochs	80
	Weight Decay	0.0005
	Dropout Rate	0.5
	Cross Validation	5-Fold

Category	Parameter	Value / Configuration
Transformer GAN	Latent Vector Dimension	100
	Attention Heads	8
	Transformer Layers	6
	Activation Function	GELU
	GAN Loss Function	Adversarial Loss
Enhanced ResNet-50	Attention Module	Squeeze-and-Excitation
	Pooling Layer	Global Average Pooling
	Final Activation	Softmax
	Output Classes	CN, MCI, AD

The selected hyperparameter configuration contributed to stable GAN convergence, improved feature representation, and enhanced classification robustness across heterogeneous MRI datasets.

4.3 Evaluation Metrics

To evaluate the performance of the proposed model in terms of the Image quality and the classification performance. We use both image quality metrics for GAN augmentation and the classification metrics.

4.3.1 Image Quality Metrics for GAN Augmentation

To evaluate the performance of the proposed GAN based model in terms of the data quality, the following metrics were used: Fréchet Inception Distance (FID): Measures similarity between the distributions of real and produced images. Lower ratings suggest more realistic outputs; Structural Similarity Index Measure (SSIM) which Evaluates structural similarity between actual and synthetic images, focusing on texture and anatomical preservation; and Peak Signal-to-Noise Ratio (PSNR) which Quantifies image reconstruction quality in terms of pixel-level fidelity.

4.3.2 Classification Metrics

To test classification performance on AD, MCI, and CN categories, the following standard measures were employed: Accuracy (ACC) which is the Overall proportion of correctly identified samples; Precision (P) which is the Ability to correctly recognize favorable predictions; Recall (R) / Sensitivity which is the Ability to appropriately identify patients with AD or MCI; Specificity (SP): Ability to appropriately identify cognitively normal subjects; F1-Score which is the Harmonic mean of Precision and Recall; and Area Under the ROC Curve (AUC) which is the Overall robustness of categorization.

5. RESULTS AND DISCUSSION

This section presents the experimental results of the proposed model. We first provide the results on the ADNI datasets and then provide the results for OASIS datasets for both the image quality based on the GAN model and the classification of the proposed approach based on the ResNet 50. Next we provide the ablation results to investigate the impact of different components of the model.

5.1 Results on ADNI Dataset

Table 3 reports the results of the proposed GAN based model compared with the baselines which include DCGAN, WGAN-GP, cGAN and StyleGAN2. The performance was evaluated based on FID, SSIM and PSNR metrics. From the table it can be observed that, The Enhanced GAN greatly outperformed the baselines, achieving the lowest FID (31.4) and the highest SSIM (0.902) and PSNR (32.8 dB).

Table 3. Image quality comparison on ADNI dataset.

Model	FID ↓	SSIM ↑	PSNR (dB) ↑
DCGAN	68.4 ± 2.1	0.781 ± 0.014	23.5 ± 0.8
WGAN-GP	54.2 ± 1.8	0.812 ± 0.012	24.7 ± 0.7
cGAN	49.6 ± 1.6	0.829 ± 0.011	25.3 ± 0.6
StyleGAN2	42.8 ± 1.3	0.853 ± 0.009	26.1 ± 0.5
Proposed Enhanced GAN	31.4 ± 0.9	0.902 ± 0.006	32.8 ± 0.4

Table 4 summarizes the classification results (including the standard deviations for 10 runs) of the proposed ResNet-50 compared with five baselines which include VGG16, DenseNet-121, 3D CNN, GAN+CNN, and Vanilla ResNet 50. Performance is expressed in terms of Accuracy (ACC), Precision (P), Recall (R), Specificity (SP), F1-Score, and AUC. From the results, one can see that, our proposed model experience an overall accuracy of 94.8% which is much higher than the vanilla ResNet-50 (87.5%) and traditional GAN+CNN techniques (86.3%). Notably, the model achieved the greatest AUC (0.97) value. Figure 6 illustrates the confusion matrices corresponding to all baseline models, providing a detailed view of their classification performance across the three classes: Normal, MCI, and AD. A progressive improvement in correct classification can be observed, particularly for the MCI and AD categories, as the quality of data augmentation increases.

Table 4. Classification performance on SDNI datasets.

Model	ACC (%)	P (%)	R (%)	SP (%)	F1 (%)	AUC
VGG16	83.2 ± 1.8	82.6 ± 1.7	80.9 ± 1.9	85.4 ± 1.5	81.7 ± 1.8	0.87 ± 0.02
DenseNet-121	85.6 ± 1.5	84.9 ± 1.4	83.1 ± 1.6	86.7 ± 1.3	84.0 ± 1.5	0.89 ± 0.01
3D CNN (Baseline)	84.1 ± 1.7	83.2 ± 1.6	82.5 ± 1.8	85.0 ± 1.5	82.8 ± 1.6	0.88 ± 0.02
GAN + CNN	86.3 ± 1.4	85.7 ± 1.3	84.2 ± 1.5	87.4 ± 1.2	84.9 ± 1.4	0.90 ± 0.01
Vanilla ResNet-50	87.5 ± 1.2	86.9 ± 1.1	85.3 ± 1.3	88.2 ± 1.0	86.1 ± 1.2	0.91 ± 0.01
Proposed ResNet-50	94.8 ± 0.7	91.8 ± 0.8	90.7 ± 0.9	93.1 ± 0.7	91.2 ± 0.8	0.97 ± 0.01

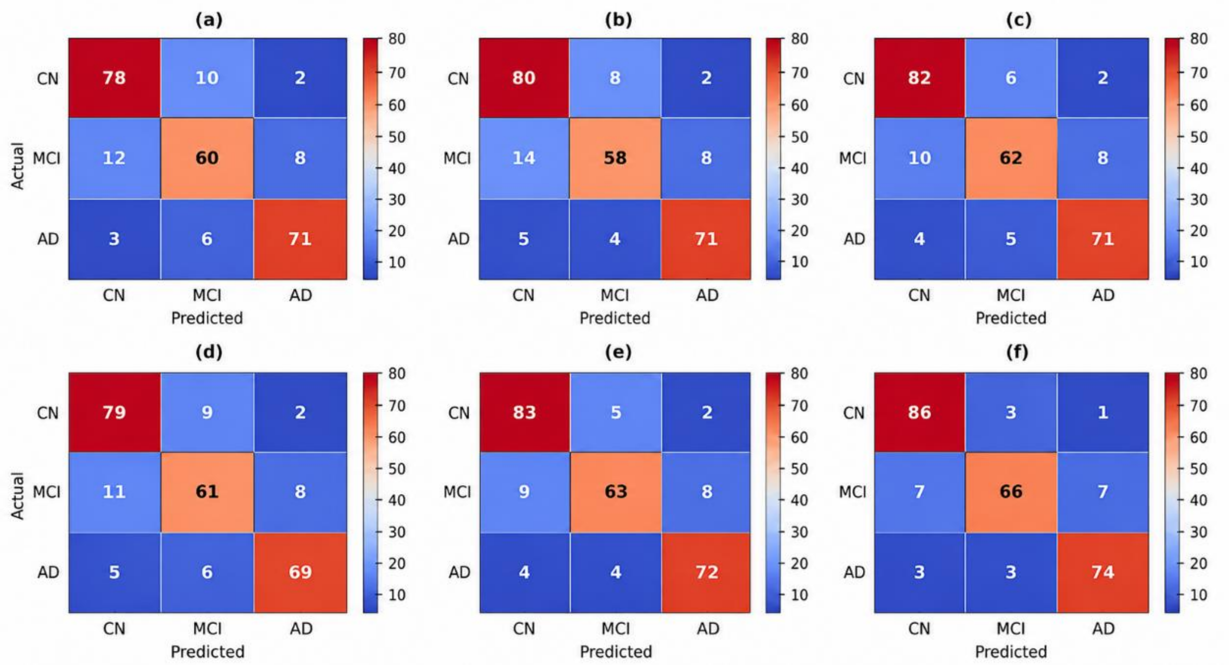

Figure 6. Confusion matrices on ADNI datasets.

The experimental results confirm the effectiveness of the proposed approach in tackling two critical challenges in AD detection: 1) Limited Data Availability in which The Enhanced GAN generated realistic and diverse MRIs, which enriches the training dataset and reduces overfitting. The Enhanced ResNet-50 captured subtle neuroanatomical differences between MCI and AD cases, outperforming all baselines in both cases. Compared to standard CNN models such as VGG16, DenseNet-121, the proposed approach delivered substantial gains in classification performances.

5.2 Results on OASIS Dataset

To validate the robustness and generalizability of the proposed framework, experiments were also conducted on the OASIS dataset. As with ADNI, performance was evaluated in two parts: (i) Image quality of generated MRIs using the proposed Enhanced GAN and (ii) Classification accuracy using the Enhanced ResNet-50 compared with baseline models. The results closely mirror those observed in ADNI. Table 5 shows the Image Quality Comparison on OASIS Dataset including the standard deviations for 10 runs. From the table, it can be shown that, the Enhanced GAN achieves the lowest FID (33.1) and the highest SSIM (0.896) and PSNR (31.9 dB) which outperforms StyleGAN2 and other baselines.

Table 5. Image quality comparison on OASIS dataset.

Model	FID ↓	SSIM ↑	PSNR (dB) ↑
DCGAN	71.2 ± 2.4	0.774 ± 0.015	22.8 ± 0.9
WGAN-GP	57.9 ± 1.9	0.801 ± 0.013	23.9 ± 0.7
cGA	51.3 ± 1.7	0.824 ± 0.011	24.6 ± 0.6
StyleGAN2	44.5 ± 1.4	0.847 ± 0.009	25.8 ± 0.5
Proposed Enhanced GAN	33.1 ± 0.8	0.896 ± 0.005	31.9 ± 0.4

https://doi.org/10.11113/humentech.v5n2.139

Table 6 shows the Classification Performance Comparison on OASIS Dataset, including the standard deviations for 10 runs. From the results it can be shown that The Enhanced ResNet-50 achieved 93.6% accuracy which outperforms the vanilla ResNet-50 (86.4%) and conventional GAN+CNN (85.2%). Importantly, the AUC of 0.9 demonstrates strong discriminative capability across AD, MCI, and CN groups. Figure 7 presents the confusion matrices for all baseline models, illustrating their classification performance across the three classes: Normal, MCI, and AD. The results highlight progressive improvements in correct classification, particularly for the MCI and AD classes, as the quality of augmentation increases.

Table 6. Classification performance comparison on OASIS dataset.

Model	ACC (%)	P (%)	R (%)	SP (%)	F1 (%)	AUC
VGG16	81.7 ± 1.9	80.9 ± 1.8	79.5 ± 2.0	83.2 ± 1.6	80.2 ± 1.8	0.85 ± 0.02
DenseNet-121	84.1 ± 1.6	83.6 ± 1.5	82.1 ± 1.7	85.3 ± 1.4	82.8 ± 1.5	0.87 ± 0.01
3D CNN (Baseline)	82.8 ± 1.8	82.1 ± 1.7	81.0 ± 1.9	84.0 ± 1.6	81.5 ± 1.7	0.86 ± 0.02
GAN + CNN (Conventional)	85.2 ± 1.5	84.6 ± 1.4	83.4 ± 1.6	86.5 ± 1.3	84.0 ± 1.4	0.88 ± 0.01
Vanilla ResNet-50	86.4 ± 1.3	85.9 ± 1.2	84.7 ± 1.4	87.2 ± 1.1	85.2 ± 1.2	0.89 ± 0.01
Enhanced ResNet-50	93.6 ± 0.8	90.5 ± 0.9	89.3 ± 1.0	92.0 ± 0.8	89.9 ± 0.9	0.96 ± 0.01

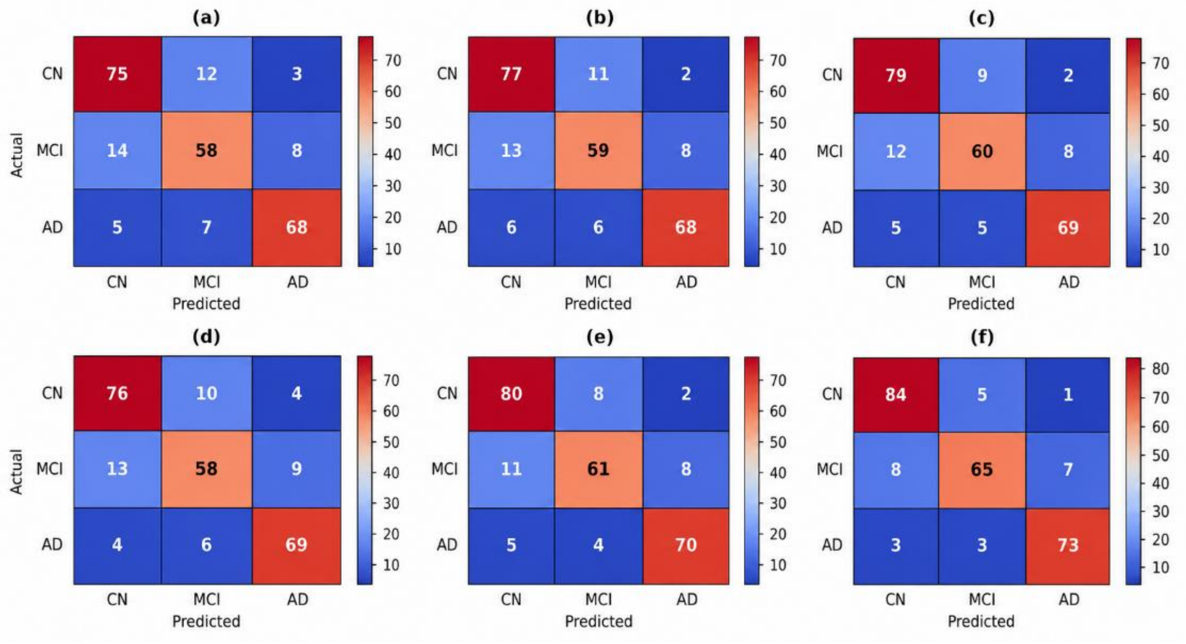

Figure 7. Confusion matrices on OASIS datasets.

The results on OASIS further confirm the robustness of the proposed framework. From the results it can be shown that, our GAN Augmentation model consistently improved data diversity and structural fidelity, as seen from high SSIM and PSNR values across both datasets. Also it can be seen that, the Classification Performance showed comparable gains in both datasets, with the Enhanced ResNet-50 maintaining superior accuracy and AUC over all baselines. Taken together, the experiments demonstrate that the proposed approach not only excels on a large-scale benchmark (ADNI) but also generalizes effectively to smaller, heterogeneous datasets (OASIS).

5.3 Comparison with State-of-the-Art Methods

To further validate the effectiveness of the proposed framework, we compare its performance with state-of-the-art data augmentation and classification approaches recently reported in literature. The evaluation is done using both image quality metrics and classification performance metrics. Table 7 shows the comparison results of the proposed GAN model. From the results it can be seen that, the proposed GAN led to superior performances in all cases. Table 8 shows the classification results with several recent deep learning-based frameworks.

From the results, it is evident that our proposed model consistently outperforms existing methods. The proposed model achieves SSIM scores of 0.902 and 0.895 on ADNI and OASIS datasets respectively. Moreover, our proposed model shows 32.8 dB and 31.9 dB on the ADNI and OASIS datasets respectively. A major strength of our model is its consistent performance across ADNI and OASIS. While most baselines show drops in SSIM or PSNR when applied to OASIS, our model maintains near-identical values across both datasets (SSIM drop of only 0.007 and PSNR drop of 0.9 dB). This indicates strong domain generalization, which is vital for real-world clinical deployment where scanners and acquisition protocols vary. Table 6 shows the effectiveness of the proposed framework against several widely adopted deep learning approaches for AD classification. From the results, we can see that the proposed model achieves 94.8% and 93.6%

accuracy on the ADNI and OASIS dataset respectively outperforming all selected baseline models. The proposed model shows absolute improvements of 2.8–4.4% on ADNI and 0.4–1.6% on OASIS. This margin, while moderate, is consistent across both datasets and demonstrates that integrating Transformer-GAN augmentation with attention mechanisms yields more discriminative features than conventional CNNs or ViT alone. ROI ensemble methods that focus on hippocampal segmentation achieve around 93–94% on OASIS, but they are limited to specific brain regions and may lose global contextual information. Similarly, GAN+CNN hybrids report accuracies in the 88–92% range with AUCs around 0.88–0.92. Our approach's AUC of 0.96–0.97 underscores its more reliable sensitivity and specificity.

Table 7. Comparison results of image quality performance.

Study	ADNI		OASIS	
	SSIM (↑)	**PSNR (↑)**	**SSIM (↑)**	**PSNR (↑)**
DSR-GAN + CNN (41)	0.847	29.3	0.841	28.8
SR GAN for Brain MRI (42)	0.944	26.92	0.940	26.1
Cross-Modality GAN (43)	0.890	N/R	0.885	N/R
Proposed (Ours)	**0.902**	**32.8**	**0.895**	**31.9**

↑ Higher is better; ↓ Lower is better; N/R = Not Reported.

Table 8. Comparison of proposed model with selected existing models.

Study	**ADNI**		**OASI**	
Model & Reference	Accuracy (%)	AUC	Accuracy (%)	AUC
(ViT + Augmentation) (44)	90.4	—	93.2	—
(Transfer Learning + Augmentation) (2, 45)	92.0	—	92.0	—
(GAN + CNN + Transfer Learning) (46)	88–92	0.88–0.92	88–92	0.88–0.92
Transformer (ViT variants) (47)	75–95	—	75–95	—
Proposed Model	94.8	0.97	93.6	0.96

6. CONCLUSION

This study proposed an enhanced framework for AD detection that integrates a TGA for data augmentation and an Enhanced ResNet-50 model for robust classification. The proposed TGAN demonstrated its ability to generate high-quality, structurally consistent synthetic MRI scans by capturing long-range dependencies and preserving critical biomarkers such as hippocampal atrophy. This augmentation significantly improved data diversity and enhanced the robustness of the classifier. The Enhanced ResNet-50 model, incorporating attention mechanisms and improved residual connections, achieved superior performance in distinguishing between Alzheimer's Disease (AD), Mild Cognitive Impairment (MCI), and Cognitively Normal (CN) subjects. Extensive experiments on ADNI and OASIS datasets confirmed that the proposed framework outperforms conventional baselines in terms of classification accuracy, sensitivity, specificity, and image quality metrics. Overall, this research demonstrates that combining Transformer-based GAN augmentation with attention-enhanced deep learning classifiers provides a powerful and generalizable solution for Alzheimer's Disease detection. Beyond AD, the methodology holds promise for other neurodegenerative disorders and broader medical imaging applications where high-quality data and reliable classification are critical. From a practical perspective, the proposed framework demonstrates strong potential as a computer-aided diagnostic support system for early-stage Alzheimer's Disease assessment using MRI data. By improving the discrimination of MCI and AD cases from cognitively normal subjects, the framework may assist clinicians in achieving more reliable and consistent diagnostic decisions. In addition, the ability of the proposed model to generalize across datasets with different imaging characteristics suggests its applicability in heterogeneous clinical environments. Despite the strong classification performance achieved by the proposed framework, interpretability and transparency remain critical considerations for real-world healthcare deployment. The proposed model combines enhanced preprocessing, Transformer-based GAN augmentation, and attention-enhanced ResNet-50 architecture, which may increase the complexity of the decision-making process. Furthermore, the use of synthetic MRI data and multiple preprocessing operations may raise concerns regarding feature reliability and potential information loss. To address these concerns, future work will incorporate Explainable Artificial Intelligence (XAI) techniques such as Grad-CAM, SHAP, and attention visualization methods to improve model interpretability. Another future direction will involve collaboration with medical specialists to perform prospective clinical validation using independent real-world MRI datasets and expert annotations.

AUTHORSHIP CONTRIBUTION STATEMENT

Ibrahem Mohammed Madhat: conceptualization, validation, formal analysis, writing—original draft preparation, supervision, funding acquisition; Farhan Mohamed: conceptualization, validation, formal analysis, supervision; Omar Albebashy: conceptualization, validation, formal analysis, writing—review and editing, project administration; Ahmed Azzawi: conceptualization, methodology, validation, formal analysis, visualization; Aminu Dau: conceptualization, software, validation, formal analysis, writing—review and editing.

DATA AVAILABILITY

Data are available upon request.

DECLARATION OF COMPETING INTEREST

The authors declare no conflict of interest.

DECLARATION OF GENERATIVE AI

The authors declare that the manuscript has been written by themselves.

REFERENCES

(1) Nagarajan I, Lakshmi Priya GG. A comprehensive review on early detection of Alzheimer's disease using various deep learning techniques. Front Comput Sci. 2025; 6:1404494. https://doi.org/10.3389/fcomp.2024.1404494
(2) Chamakuri R, Janapana H. A systematic review on recent methods on deep learning for automatic detection of Alzheimer's disease. Med Nov Technol Devices. 2025; 25:100343. https://doi.org/10.1016/j.medntd.2024.100343
(3) Toumaj S, Heidari A, Shahhosseini R, Jafari Navimipour N. Applications of deep learning in Alzheimer's disease: A systematic literature review of current trends, methodologies, challenges, innovations, and future directions. Artif Intell Rev. 2024; 58(2):44. https://doi.org/10.1007/s10462-024-11041-5.
(4) Akan T, Oskouei AG, Alp S, Bhuiyan MAN. Brain magnetic resonance image (MRI) segmentation using multimodal optimization. Multimed Tools Appl. 2025; 84(16):16971–17020. https://doi.org/10.1007/s11042-024-19725-4.
(5) Ávila-Jiménez JL, Cantón-Habas V, Carrera-González MP, Rich-Ruiz M, Ventura S. A deep learning model for Alzheimer's disease diagnosis based on patient clinical records. Comput Biol Med. 2024; 169:107814. https://doi.org/10.1016/j.compbiomed.2023.107814.
(6) Marino C, Perez-Corredor P, O'Hare M, Heuer A, Chmielewska N, Gordon H, Chandrahas AS, Gonzalez-Buendia L, Delgado-Tirado S, Doan TH, Vanderleest TE, Arevalo-Alquichire S, Obar RA, Ortiz-Cordero C, Villegas A, Sepulveda-Falla D, Kim LA, Lopera F, Mahley R, Huang Y, Quiroz YT, Arboleda-Velasquez JF. The Alzheimer's Disease Neuroimaging Initiative in the era of Alzheimer's disease treatment: A review of ADNI studies from 2021 to 2022. Alzheimers Dement. 2024; 20(1):652–694 https://doi.org/10.1002/alz.13436.
(7) Basheer S, Bhatia S, Sakri SB. Computational modeling of dementia prediction using deep neural network: Analysis on OASIS dataset. IEEE Access. 2021; 9:42449–42462. https://doi.org/10.1109/ACCESS.2021.3066213 https://doi.org/10.1109/ACCESS.2021.3066213
(8) De Souza VLT, Marques BAD, Batagelo HC, Gois JP. A review on generative adversarial networks for image generation. Comput Graph. 2023; 114:13–25. https://doi.org/10.1016/j.cag.2023.05.010
(9) Krichen M. Generative adversarial networks. Proceedings of the 14th International Conference on Computing Communication and Networking Technologies (ICCCNT). IEEE; 2023. 1–7. https://doi.org/10.1109/ICCCNT56998.2023.10306417
(10) Egger J, Gsaxner C, Pepe A, Pomykala KL, Jonske F, Kurz M, Li J, Kleesiek J. Medical deep learning—A systematic meta-review. Comput Methods Programs Biomed. 2022; 221:106874. https://doi.org/10.1016/j.cmpb.2022.106874
(11) Koonce B, Koonce B. ResNet 50. Convolutional Neural Networks with Swift TensorFlow: Image Recognition and Dataset Categorization. 2021. 63–72. https://doi.org/10.1007/978-1-4842-6168-2_6
(12) Salehi AW, Khan S, Gupta G, Alabduallah BI, Almjally A, Alsolai H, Siddiqui T, Mellit A.. A study of CNN and transfer learning in medical imaging: Advantages, challenges, future scope. Sustainability. 2023; 15(7):5930. https://doi.org/10.3390/su15075930
(13) Oraby S, Emran A, El-Saghir B, Mohsen S. Hybrid of DSR-GAN and CNN for Alzheimer disease classification. Sci Rep. 2025. https://doi.org/10.1038/s41598-025-94677-9
(14) AbdulAzeem Y, Bahgat WM, Badawy M. A CNN based framework for classification of Alzheimer's disease. Neural Comput Appl. 2021; 33(16):10415–10428. https://doi.org/10.1007/s00521-021-05799-w.
(15) Al-Khuzaie FEK, Bayat O, Duru AD. Diagnosis of Alzheimer's disease using 2D MRI slices by convolutional neural network. Appl Bionics Biomech. 2021:1–9. https://doi.org/10.1155/2021/6690539
(16) Al-Adhaileh MH. Diagnosis and classification of Alzheimer's disease by using a convolution neural network algorithm. Soft Comput. 2022; 26:7751–7762. https://doi.org/10.1007/s00500-022-06762-0
(17) Antony F, Anita HB, George JA. Classification on Alzheimer's disease MRI images with VGG-16 and VGG-19. In: Lecture Notes in Networks and Systems. Vol. 312. Singapore: Springer; 2023. https://doi.org/10.1007/978-981-19-3575-6_22
(18) Savaş S. Detecting the stages of Alzheimer's disease with pre-trained deep learning architectures. Arab J Sci Eng. 2022; 47(2):2201–2218. https://doi.org/10.1007/s13369-021-06131-3
(19) Sarasua I, Pölsterl S, Wachinger C. Hippocampal representations for deep learning on Alzheimer's disease. Sci Rep. 2022;12:8619. https://doi.org/10.1038/s41598-022-12533-6
(20) Cui R, Liu M. Ensemble of 3D densely connected convolutional network for diagnosis of mild cognitive impairment and Alzheimer's disease. Neurocomputing. 2019;333:145–156. https://doi.org/10.1016/j.neucom.2018.12.018.
(21) Ebrahimi A, Luo S, Chiong R. Introducing transfer learning to 3D ResNet-18 for Alzheimer's disease detection on MRI images. In: 2020 35th International Conference on Image and Vision Computing New Zealand. IEEE; 2020:1–6. https://doi.org/10.1109/IVCNZ51579.2020.9290616.

(22) Khan R, Akbar S, Mehmood A, Shahid F, Munir K, Ilyas N, Asif M, Zheng Z. A transfer learning approach for multiclass classification of Alzheimer's disease using MRI images. Front Neurosci. 2023;16:1050777. https://doi.org/10.3389/fnins.2022.1050777.
(23) Qu C, Zou Y, Ma Y, Chen Q, Luo J, Fan H, Jia Z, Gong Q, Chen T. Diagnostic performance of generative adversarial network-based deep learning methods for Alzheimer's disease. Front Aging Neurosci. 2022; 14. https://doi.org/10.3389/fnagi.2022.841696
(24) Jenkins J, Roy K. Exploring deep convolutional generative adversarial networks (DCGAN) in biometric systems: A survey study. Discov Artif Intell. 2024; 4(1):42. https://doi.org/10.1007/s44163-024-00138-z.
(25) Abdelhalim ISA, Mohamed MF, Mahdy YB. Data augmentation for skin lesion using self-attention based progressive generative adversarial network. Expert Syst Appl. 2021; 165:113922. https://doi.org/10.1016/j.eswa.2020.113922
(26) Melnik A, Miasayedzenkau M, Makarovets D, Pirshtuk D, Akbulut E, Holzmann D, Renusch T, Reichert G, Ritter H. Face generation and editing with StyleGAN: A survey. IEEE Trans Pattern Anal Mach Intell. 2024; 46(5):3557–3576. https://doi.org/10.1109/TPAMI.2023.3336805
(27) Elloumi N, Seddik H. The ideal PGGAN for the 3D medical data segmenting. Proceedings of the 2024 IEEE 7th International Conference on Advanced Technologies, Signal and Image Processing (ATSIP). IEEE; 2024. 665–675. https://doi.org/10.1109/ATSIP62566.2024.10638946.
(28) Purwono P, Wulandari ANE, Ma'arif A, Salah WA. Understanding generative adversarial networks (GANs): A review. Control Syst Optim Lett. 2025; 3(1):36–45. https://doi.org/10.59247/csol.v3i1.170.
(29) Akter S. Generative AI: A Pix2Pix-GAN-based machine learning approach for robust and efficient lung segmentation. arXiv [Preprint]. 2024; arXiv:2412.10826. Available from: https://doi.org/10.48550/arXiv.2412.10826.
(30) Ferdousi J, Lincoln SI, Alom MK, Foysal M. A deep learning approach for white blood cells image generation and classification using SRGAN and VGG19. Telemat Inform Rep. 2024; 16:100163. https://doi.org/10.1016/j.teler.2024.100163
(31) Lee J, Nishikawa RM. Improving lesion detection in mammograms by leveraging a Cycle-GAN-based lesion remover. Breast Cancer Res. 2024; 26(1):21. https://doi.org/10.1186/s13058-024-01777-x.
(32) Cai Y, Li Y, Zhang Z. Comprehensive study and analysis for StarGAN and StarGAN-v2 in the task of image generation. J Phys Conf Ser. IOP Publishing; 2023. 12049. https://doi.org/10.1088/1742-6596/2634/1/012049.
(33) Oraby O, El-Shafai M, Saleh MH. DSR-GAN for Alzheimer's disease MRI augmentation and classification. Comput Med Imaging Graph. 2023. https://doi.org/10.1038/s41598-025-94677-9.
(34) Paul S, Chen PY. Vision transformers are robust learners. Proceedings of the AAAI Conference on Artificial Intelligence. 2022. 2071–2081. https://doi.org/10.48550/arXiv.2105.07581.
(35) Gogianu F, Berariu T, Rosca MC, Clopath C, Busoniu L, Pascanu R. Spectral normalisation for deep reinforcement learning: An optimisation perspective. Proceedings of the International Conference on Machine Learning. PMLR; 2021. 3734–3744. https://proceedings.mlr.press/v139/gogianu21a.html
(36) Paszke A, Gross S, Massa F, Lerer A, Bradbury J, Chanan G, Killeen T, Lin Z, Gimelshein N, Antiga L, Desmaison A, Köpf A, Yang E, DeVito Z, Raison M, Tejani A, Chilamkurthy S, Steiner B, Fang L, Bai J, Chintala S. PyTorch: An imperative style, high-performance deep learning library. Advances in Neural Information Processing Systems. 2019. 8024–8035. https://doi.org/10.48550/arXiv.1912.01703.
(37) Abadi M, Barham P, Chen J, Chen Z, et al. TensorFlow: A system for large-scale machine learning. Proceedings of the 12th USENIX Symposium on Operating Systems Design and Implementation (OSDI). 2016. 265–283. https://doi.org/10.48550/arXiv.1605.08695.
(38) Kingma DP, Ba JL. Adam: A method for stochastic optimization. Proceedings of the 3rd International Conference on Learning Representations (ICLR). 2015. 1–15. https://doi.org/10.48550/arXiv.1412.6980
(39) Jack CR, Bernstein M, Fox N, et al. The Alzheimer's Disease Neuroimaging Initiative (ADNI): MRI methods. J Magn Reson Imaging. 2008;27(4):685–691. https://doi.org/10.1002/jmri.21049
(40) LaMontagne PJ, Benzinger TLS, Morris JC, Keefe S, Hornbeck R, Xiong C, Grant E, Hassenstab J, Moulder K, Vlassenko AG, Raichle ME, Cruchaga C, Marcus D. OASIS-3: Longitudinal neuroimaging, clinical, and cognitive dataset for normal aging and Alzheimer disease. medRxiv. 2019. https://doi.org/10.1101/2019.12.13.19014902
(41) Oraby S, Emran A, El-Saghir B, Mohsen S. Hybrid of DSR-GAN and CNN for Alzheimer disease detection based on MRI images. Sci Rep. 2025; 15:12727. https://www.nature.com/articles/s41598-025-94677-9
(42) Ikuta K, Iyatomi H, Oishi K. Super-resolution for brain MR images from a significantly small amount of training data. Comput Sci Math Forum. 2022;3(1):7. https://doi.org/10.3390/cmsf2022003007
(43) Hassanzadeh R, Abrol A, Hassanzadeh HR, Calhoun VD. Cross-modality translation with GANs to unveil Alzheimer's disease biomarkers [Internet]. arXiv Prepr. 2024 [cited 2026 Jun 3]. Available from: https://arxiv.org/abs/2405.05462
(44) Lazli L. Improved Alzheimer disease diagnosis with a machine learning approach and neuroimaging: Case study development. JMIRx Med. 2025; 6. https://doi.org/10.2196/60866
(45) Ghosh T, Palash MIA, Yousuf MA, Hamid MA, Monowar MM, Alassafi MO. A robust distributed deep learning approach to detect Alzheimer's disease from MRI images. Mathematics. 2023;11(12):2633. https://doi.org/10.3390/math11122633
(46) Chui KT, Gupta BB, Alhalabi W, Alzahrani FS. An MRI scans-based Alzheimer's disease detection via convolutional neural network and transfer learning. Diagnostics. 2022;12(7):1531. https://doi.org/10.3390/diagnostics12071531
(47) Wang Y, Chen K, Zhang Y, Wang H. MedTransformer: Accurate Alzheimer's disease diagnosis for 3D MRI images through 2D vision transformers. arXiv Prepr. 2024. https://doi.org/10.48550/arXiv.2401.06349